Computational Mechanics 26 (2000) 566–570 © Springer-Verlag 2000

Calculating the energy-norm FEM-error for Reissner–Mindlin plates without known reference solution

C. Carstensen, K. Weinberg

Abstract The validation of (recently introduced conforming) finite element technologies for the numerical treatment of Reissner–Mindlin plate models requires comparisons with the unknown exact solution. Since mathematical results are often provided for the error in energy norms only it is not sufficient to compare a typical displacement or moment at one point of the domain. Instead of computing a reference solution on a very fine mesh (and then providing a lot of data for the public) we propose the storage of one (problem depending) constant C which then allows an error representation which merely involves known quantities. Based on this approach we could verify convergence rates which were theoretically predicted and give experimental evidence that new adaptive automatic mesh-refining algorithms yield superior approximations. Given any reasonable guess of C (computable from known quantities), our error representation yields an approximation for the unknown error. This establishes a method for a posteriori error control to be employed as a termination criterion.

1 Introduction

Mixed finite element schemes in general require deeper mathematical analysis as an arbitrary choice of ansatz and test spaces yields instabilities. Very recently, new finite element methods where introduced in the mathematical literature [1, 2, 3, 6, 8] for the effective numerical treatment of the Reissner–Mindlin model of the moderately thick plate

$$t^2 \mathrm{div}\left(\frac{\lambda}{12}\mathbb{I}\,\mathrm{div}\,\vartheta + \frac{\mu}{6}\varepsilon(\vartheta)\right) + \mu(\nabla w - \vartheta) = 0 \ , \quad (1.1)$$

$$\mu\,\mathrm{div}(\nabla w - \vartheta) + f = 0 \ . \quad (1.2)$$

Received 9 May 2000

C. Carstensen
Mathematisches Seminar,
Christian-Albrechts-Universität zu Kiel Ludewig-Meyn-Str. 4,
D-24098 Kiel, FRG

K. Weinberg (✉)
Institut füer Mathematik, Medizinische Universität zu Lübeck,
Wallstr. 40, D-23560 Lübeck, FRG

The second author (K.W.) thankfully acknowledges partial support by the German Research Foundation (DFG) within the Graduiertenkolleg 'Effiziente Algorithmen und Mehrskalenmethoden'.

The numerical verification of the theoretically predicted convergence rates for those schemes is either missing or problematic: The relation to the Kirchhoff plate model is employed in [6], but restricted to very thin plates where (1.1)–(1.2) is not designed for. The influence of the important parameter α (cf. below) is studied in [2] only by comparing one typical displacement (whose convergence properties were not covered by the theory). The superiority of adaptive mesh-refining algorithms could not be shown experimentally in [10] because of the lack of a typical singular example with known reference solution.

The design of a benchmark with known exact solution to (1.1)–(1.2) is difficult: prescribing a general vertical displacement w and rotations $\vartheta = (\vartheta_1, \vartheta_2)$ of the plate normal does not necessarily satisfy (1.1) (while we could choose f to satisfy (1.2)). Even more problematic is a typical choice of (w, ϑ) which reflects the finite element's performance in practise.

Our work was motivated by a strange pre-asymptotic performance of recent finite elements in [10] which rather suggested errors in our code than the predicted linear convergence. Here, we establish an error representation for the energy norm ($\|\cdot\|$ denotes the norm in the Lebesgue space $L^2(\Omega)$)

$$e_h^2 := \| \mathbb{C}^{1/2}\varepsilon(\vartheta - \vartheta_h) \|^2 + t^{-2} \| \vartheta - \vartheta_h - \nabla(w - w_h) \|^2 = C + \text{computable terms } (w_h, \vartheta_h) \ . \quad (1.3)$$

The constant C could be computed from f and the unknown w. In practise we may use a finite element calculation on a very fine mesh to provide this constant C and then may use the second identity in (1.3) to calculate e_h. Notice that we need to calculate C only once and thereafter everybody could use our error representation to calculate e_h on a different mesh with different conforming finite elements.

Given an approximation C_h to C, obtained, e.g., by extrapolation techniques from computed moderately fine meshes, we can use (1.3) to calculate

$$\eta_h^2 := C_h + \text{computable terms } (w_h, \vartheta_h) \quad (1.4)$$

as an approximation to e_h which may serve as an a posteriori termination criterion. Numerical evidence for the efficiency of the error estimator η_h is provided.

The rest of the paper is organised as follows: Detailed notations, weak and discrete formulations are provided in Sect. 2. Our theoretical main result is stated and proven in Sect. 3. The first example of Sect. 4 compares our results with an analytical solution for the Kirchhoff equation on a square plate while the second of Sect. 5 illustrates the practical application of the strategy proposed. As a result

we can establish theoretical predicted convergence rates and superiority of the adaptive algorithm from [5] over a uniform refinement by numerical experiments.

2
Weak formulation and finite element discretisation

The strong formulation (1.1)–(1.2) with the identity matrix $\mathbb{I}$, the two-dimensional linear Green strain tensor $\varepsilon(\vartheta) = \mathrm{sym}(\nabla\vartheta)$ is recast with a scaled external load $g := f/(\mu k t^2)$ and elasticity tensor $\mathbb{C}$, $\mathbb{C}\varepsilon = \lambda/(12\mu k)\mathbb{I}\,\mathrm{tr}\,\varepsilon + \varepsilon/(6k)$, with constant material coefficients μ, λ, shear correction factor k and constant plate thickness t. In its weak formulation the problem reads: Find $(w,\vartheta) \in H_0^1(\Omega) \times H_0^1(\Omega)^2$ such that, for all $(v,\varphi) \in H_0^1(\Omega) \times H_0^1(\Omega)^2$,

$$(\varepsilon(\vartheta); \mathbb{C}\varepsilon(\varphi)) + t^{-2}(\nabla w - \vartheta; \nabla v - \varphi) = (g; w) \ . \tag{2.1}$$

The Sobolev space $H_0^1(\Omega)$ contains all functions with a square-integrable gradient and homogeneous boundary conditions and $(\cdot;\cdot)$ denotes the $L^2(\Omega)$-scalar product: $(g; w) = \int_\Omega w \cdot g \,\mathrm{d}x$.

Because of the shear locking phenomena the finite element discretisation of (2.1) is not trivial. To rewrite (2.1) as a saddle point problem we follow Arnold and Brezzi [1] and introduce a shear variable

$$\gamma := (t^{-2} - \alpha)(\nabla w - \vartheta) \text{ for a parameter } \alpha \text{ with}$$
$$0 \le \alpha = \alpha(x) < t^{-2} \ . \tag{2.2}$$

In this paper, the function $\alpha = \alpha(x)$ is a possibly discontinuous function which may vary with $x \in \Omega$ and may be different on different elements. We suppose that $0 \le \alpha < t^{-2}$ is bounded away from t^{-2} such that $(t^{-2} - \alpha)^{-1}$ is essentially bounded. With bilinear forms

$$a(w,\vartheta; v,\varphi) := (\varepsilon(\vartheta); \mathbb{C}\varepsilon(\varphi)) + (\alpha(\nabla w - \vartheta); \nabla v - \varphi) \ , \tag{2.3}$$

$$b(w,\vartheta;\eta) := (\nabla w - \vartheta; \eta) \ , \tag{2.4}$$

$$c(\gamma;\eta) := (t^2/(1-\alpha t^2)\gamma; \eta) \ , \tag{2.5}$$

the continuous problem reads: Find $(w,\vartheta,\gamma) \in H_0^1(\Omega) \times H_0^1(\Omega)^2 \times L^2(\Omega)^2$ such that

$$a(w,\vartheta; v,\varphi) + b(v,\varphi;\gamma) = (g; v) \ , \tag{2.6}$$

$$b(w,\vartheta;\eta) - c(\gamma;\eta) = 0 \tag{2.7}$$

for all $(v,\varphi,\eta) \in H_0^1(\Omega) \times H_0^1(\Omega)^2 \times L^2(\Omega)^2$.

The conforming discretisation is described by replacing the continuous spaces $H_0^1(\Omega) \times H_0^1(\Omega)^2 \times L^2(\Omega)^2$ by subspaces $\mathscr{H}_w \times \mathscr{H}_\vartheta \times \mathscr{L}_\gamma \subset H_0^1(\Omega) \times H_0^1(\Omega)^2 \times L^2(\Omega)^2$ which are based on a mesh $\mathscr{T}$ (we neglect the subindex h for simplicity).

Suppose $\mathscr{T}$ to be a regular triangulation in the sense of Ciarlet [7], i.e. $\mathscr{T}$ is a finite partition of Ω into closed triangles $T_1, T_2, \ldots, T_n$. Let $\mathscr{P}_k(\mathscr{T})$ be the linear space of $\mathscr{T}$-piecewise polynomials of degree $\le k$,

$$\mathscr{P}_k(\mathscr{T}) := \left\{ u \in L^2(\Omega) : \forall\, T \in \mathscr{T}, u|_T \in \mathscr{P}_k(T) \right\} \ , \tag{2.8}$$

and let $\mathscr{B}_3(\mathscr{T})$ be the space of $\mathscr{T}$-piecewise cubic bubble functions,

$$\mathscr{B}_3(\mathscr{T}) := \left\{ u \in C(\Omega) : \forall\, T \in \mathscr{T}, u|_T \in \mathscr{P}_3 \right.$$
$$\left. \text{and } u = 0 \text{ on } \partial T \right\} \ . \tag{2.9}$$

Then, after Arnold and Brezzi [1], the following finite element scheme with $\mathscr{T}$-piecewise quadratic polynomials for the transverse displacement, $\mathscr{T}$-piecewise affines plus bubble modes for the rotation components, and $\mathscr{T}$-piecewise constants for the shear variable components,

$$\mathscr{H}_w \times \mathscr{H}_\vartheta \times \mathscr{L}_\gamma$$
$$:= (\mathscr{P}_2(\mathscr{T}) \cap H_0^1(\Omega))((\mathscr{P}_1(\mathscr{T}) \oplus \mathscr{B}_3(\mathscr{T})) \cap H_0^1(\Omega))^2$$
$$\times \mathscr{P}_0(\mathscr{T})^2 \ , \tag{2.10}$$

yields a stable discrete problem which reads: Find $(w_h, \vartheta_h, \gamma_h) \in \mathscr{H}_w \times \mathscr{H}_\vartheta \times \mathscr{L}_\gamma$ such that

$$a(w_h,\vartheta_h; v_h,\varphi_h) + b(v_h,\varphi_h;\gamma_h) = (g; v_h) \ , \tag{2.11}$$

$$b(w_h,\vartheta_h;\eta_h) - c(\gamma_h;\eta_h) = 0 \ , \tag{2.12}$$

for all $(v_h,\varphi_h,\eta_h) \in \mathscr{H}_w \times \mathscr{H}_\vartheta \times \mathscr{L}_\gamma$.

3
Error representation

The error representation (1.3) is established below where $(w,\vartheta) \in H_0^1(\Omega) \times H_0^1(\Omega)^2$ denotes the exact solution to (1.1)–(1.2) and $(w_h,\vartheta_h) \in \mathscr{H}_w \times \mathscr{H}_\vartheta$ solves (2.11)–(2.12). Then, the right-hand side of (3.1) specifies what is called "computable terms (w_h,ϑ_h)" in the introduction.

Theorem 1. *With the real number*
$C := (g; w) = \| \mathbb{C}^{1/2}\varepsilon(\vartheta) \|^2 + t^{-2} \| \vartheta - \nabla w \|^2$ *we have*

$$\| \mathbb{C}^{1/2}\varepsilon(\vartheta - \vartheta_h) \|^2 + t^{-2} \| \vartheta - \vartheta_h - \nabla(w - w_h) \|^2$$
$$= C - \| \mathbb{C}^{1/2}\varepsilon(\vartheta_h) \|^2 - t^{-2} \| \nabla w_h - \vartheta_h \|^2$$
$$+ 2((t^{-2} - \alpha)(\nabla w_h - \vartheta_h) - \gamma_h; \nabla w_h - \vartheta_h) \ . \tag{3.1}$$

Remark 1. The theorem holds for mixed boundary conditions as well with the only modification that, then, $C = \| \mathbb{C}^{1/2}\varepsilon(\vartheta) \|^2 + t^{-2} \| \vartheta - \nabla w \|^2$ equals the total exterior energy of the exact solution (which inludes $(g; w)$ and other energy contributions on the boundary). The theorem holds for other conforming finite element schemes, for all inhomogeneous parameters $\alpha(x)$, and arbitrary meshes as well with the same (t-depending) constant C.

Proof. Abbreviate the discretisation errors $e_w := w - w_h$ and $e_\vartheta := \vartheta - \vartheta_h$ and calculate

$$\| \mathbb{C}^{1/2}\varepsilon(e_\vartheta) \|^2 + t^{-2} \| \nabla e_w - e_\vartheta \|^2$$
$$= (\varepsilon(e_\vartheta); \mathbb{C}\varepsilon(\vartheta + \vartheta_h)) - 2(\varepsilon(e_\vartheta); \mathbb{C}\varepsilon(\vartheta_h))$$
$$+ t^{-2}(e_\vartheta - \nabla e_w; \vartheta + \vartheta_h - \nabla w - \nabla w_h)$$
$$- 2t^{-2}(e_\vartheta - \nabla e_w, \vartheta_h - \nabla w_h)$$
$$= \| \mathbb{C}^{1/2}\varepsilon(\vartheta) \|^2 + t^{-2} \| \vartheta - \nabla w \|^2$$
$$+ \| \mathbb{C}^{1/2}\varepsilon(\vartheta_h) \|^2 + t^{-2} \| \vartheta_h - \nabla w_h \|^2$$
$$- 2(\varepsilon(\vartheta); \mathbb{C}\varepsilon(\vartheta_h)) - 2t^{-2}(\vartheta - \nabla w; \vartheta_h - \nabla w_h) \ . \tag{3.2}$$

The weak form (2.7) implies (2.2) and the difference of (2.6) and (2.11) yields

$$(\varepsilon(e_\vartheta); \mathbb{C}\varepsilon(\vartheta_h)) = -(\gamma - \gamma_h + \alpha(\nabla e_w - e_\vartheta); \nabla w_h - \vartheta_h) \ . \tag{3.3}$$

Then, direct calculations show that (3.2) equals C plus

$$-\| \mathbb{C}^{1/2}\varepsilon(\vartheta_h) \|^2 - t^{-2} \| \vartheta_h - \nabla w_h \|^2 + 2((t^{-2} - \alpha)(\nabla w_h - \vartheta_h) - \gamma_h; \nabla w_h - \vartheta_h) \ . \tag{3.4}$$

The representation of C as the exterior work follows with $v = w$ and $\varphi = \vartheta$ in (2.6)–(2.7). □

Based on the identity (3.1), we proposed the following procedures on the computation of e_h resp. η_h.

(i) For a sequence $(\mathscr{T}_k)$ of uniformly refined meshes compute the discrete displacement (w_{h_k}) and calculate $C_{h_k} := (g; w_{h_k})$. Compute C by extrapolation of the sequence (C_{h_k}). (Alternatively, compute C from an analytical solution or with a numerical reference solution on a very fine mesh.) Step (i) has to be performed once for an example and is determined by Ω, g and t.

(ii) For any (known) discrete solution (w_h, ϑ_h) from any conforming finite element scheme on any mesh, compute

$$C - \| \mathbb{C}^{1/2}\varepsilon(\vartheta_h) \|^2 - t^{-2} \| \nabla w_h - \vartheta_h \|^2 + 2((t^{-2} - \alpha)(\nabla w_h - \vartheta_h) - \gamma_h; \nabla w_h - \vartheta_h) \tag{3.5}$$

which then is (an approximation up to computer precision and errors in C to) e_h^2.

Subsequent tests can take C from the literature and merely implement step (ii).

(iii) Steps (i)–(ii) can be linked to compute η_h for a posteriori error control in actual computations on at minimal three consecutive meshes, e.g., within an adaptive mesh-refining algorithm: For each sequence of three consecutive successively refined meshes $\mathscr{T}_1, \mathscr{T}_2, \mathscr{T}_3$ compute the corresponding discrete solutions $(w_1, \vartheta_1, \gamma_1)$, $(w_2, \vartheta_2, \gamma_2)$, $(w_3, \vartheta_3, \gamma_3)$ and the parameters $c_1 := (g; w_1)$, $c_2 := (g; w_2)$, $c_3 := (g; w_3)$. With Aitken-Δ^2-extrapolation method [9] consider $C_h := c_1 - (c_2 - c_1)^2/(c_3 - 2c_2 + c_1)$ (or C_h provided by any other extrapolation scheme) as an improved approximation to $C = (w; g)$. Given C_h and $(w_h, \vartheta_h) := (w_3, \vartheta_3)$ employ (1.4) to compute η_h as a known approximation to the (unknown) energy error e_h of (w_h, ϑ_h).

4
Example for comparison with Kirchhoff solution

Since the solutions of (1.1)–(1.2) tend (in a very weak topology) to the solutions of Kirchhoff's equations when $t \to 0$, we compare our computation of C with the exact value $(g; w)$ for the (different) solution w defined, for $(x, y) \in \Omega := (-1/2, +1/2)^2$, by

$$w(x, y) = (x - 1/2)^2(x + 1/2)^2(y - 1/2)^2(y + 1/2)^2 \ , \tag{4.1}$$

and with $f = t^2/12(\lambda + 2\mu)\Delta\Delta w$, $\mu = 4.2$, $\lambda = 3.6$ and a thickness of $t = 0.001$. Given (4.1) we obtained $(g; w) = 2.3323615 \cdot 10^{-10}$ as an approximation to the unknown C in (1.3) for the original Eqs. (1.1)–(1.2).

Using symmetry we calculated only one quarter $[0, 0.5]^2$ of the domain Ω. The first mesh $\mathscr{T}_1$ consisted of 4 squares each divided into 2 triangles with $N = 52$ degrees of freedom. Table 1 displays the results from uniform mesh refinements and $\alpha = 100$ where the errors e_h were computed with (1.3) for $C = 2.3324 \cdot 10^{-10}$ in every refinement step k, $e_h =: e_k$. The last two columns of Table 1 show the two error terms computed analytically with w from (4.1). As the last column has to be multiplied by $t^{-2} = 10^6$ and added to the second last, the digits of the last column agree very nicely with e_h^2 computed as proposed in this paper.

In this example, the reference solution provided an accurate approximation for the constant C. To illustrate the quality of the Aitken-Δ^2-method [9], we computed the entries in the third column of Table 1 called $(c_1, \ldots, c_6)$ by $c_k := (g; w_k)$ where w_k is (part of) the discrete solution on the mesh $\mathscr{T}_k$. The transformation

$$C_k = c_{k-2} - \frac{(c_{k-1} - c_{k-2})^2}{c_k - 2c_{k-1} + c_{k-2}} \tag{4.2}$$

provided the numbers $(C_3, \ldots, C_6)$ displayed in the third column in Table 1. One important experimental observation of this note is that the extrapolated quantities are apparently very accurate approximations to the exact value C and this yields a very good a posteriori error estimation by η_h computed as described in (iii) of the previous section.

Given that $c_1, \ldots, c_k$ are known (with $k \geq 3$) we replaced C_h in (1.4) by the extrapolated value (4.2) to compute $\eta_h =: \eta_k$ shown in the sixth column of Table 1.

To study convergence rates of the finite element scheme (2.10) for different values of α, the relative error $e_N := e_h/\sqrt{C}$ is computed as before and plotted in Fig. 1. Here and below the error e_N is plotted versus the number of degrees of freedom N in a log/log-scale; whence a slope $-1/2$ in the figures below corresponds to an experimental convergence rate 1 owing to $N \propto h^{-2}$ in two dimensions. For comparisons, triangles with slops 1 and 3/2 are shown in the figure as well.

Table 1. Numerical results in the Example of Sect. 4 for uniform mesh-refinements and $\alpha = 100$

k	N	$c_k \times 10^{-10}$	$e_k \times 10^{-5}$	$C_k \times 10^{-10}$	$\eta_k \times 10^{-5}$	$\|\|\mathbb{C}^{1/2}\varepsilon(e_\vartheta)\|\|^2 \times 10^{-16}$	$\|\|e_\vartheta - \nabla e_w\|\|^2 \times 10^{-16}$
1	52	1.6489	42.506			150.34	1806.3
2	216	2.1773	14.318			39.966	204.88
3	880	2.2979	4.4645	2.3336	4.4646	9.7138	19.899
4	3552	2.3242	1.6968	2.3315	1.6965	2.3925	2.8712
5	14272	2.3304	0.77933	2.3323	0.77930	0.59327	0.60501
6	57216	2.3319	0.38257	2.3324	0.38259	0.14765	0.14641

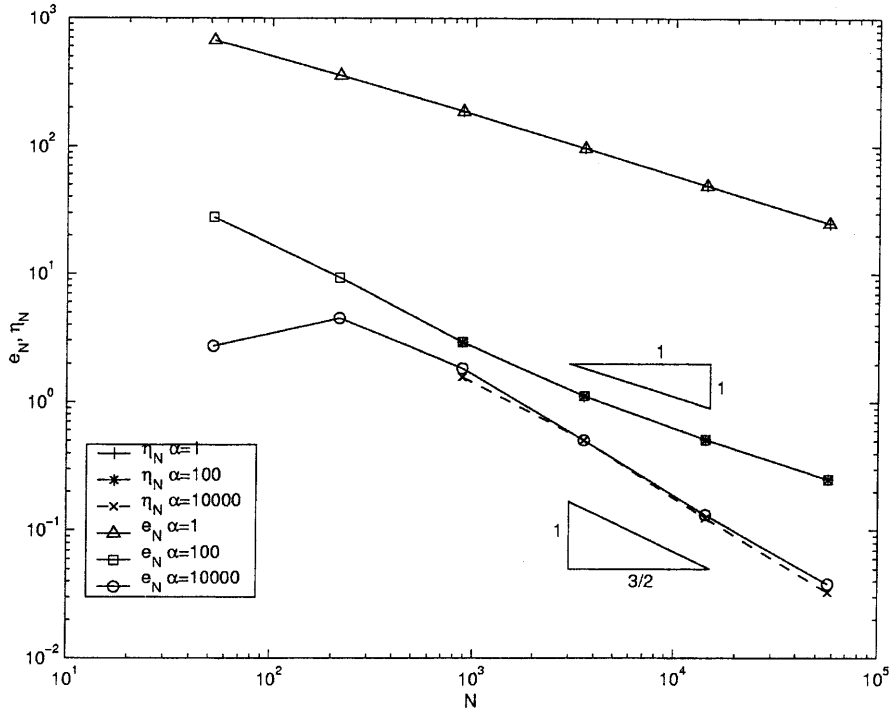

Fig. 1. Relative error versus number of degrees of freedom N for various α in the example of Sect. 4

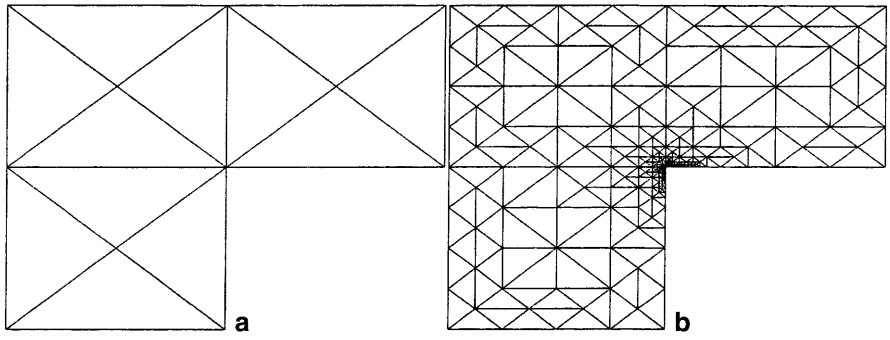

Fig. 2a,b. Finite element meshes in the example of Sect. 5. **a** initial mesh τ_0, **b** adaptive refined mesh τ_g

We observe in Fig. 1 that α influences the relative error dramatically. The results for $\alpha = 1$ yield the theoretically predicted convergence rate 1, while the convergence for $\alpha = 100$ and $\alpha = 10^4$ partially are improved. We remark that the slopes for $\alpha = 100$ are nearly 3/2 for the first four meshes and 1 for the last two. Theoretical investigations suggest an improved rate of 3/2 if $\alpha = O(h)$ [2].

The experimental convergence rate for $\alpha = 10^4$ is approximately 2 while in the pre-asymptotic range (e.g., the first entry) we even observe a non-monotone (whence non-systematic) error behaviour. Improved convergence results for smaller α were theoretically predicted in [6].

To assess the quality of the a posteriori error estimator η_h, as described in (ii) of Sect. 4, the relative error estimators $\eta_N := \eta_k/\sqrt{C_k}$ are plotted in Fig. 1 (for $k = 3, \ldots, 6$). The entries for e_k and η_k lay on top of each other which is numerical evidence for a high accuracy of the proposed error estimation.

5
Numerical example for practical error computation

Consider the L-shaped plate $(-1,1)^2 \backslash [0,1]^2$ of thickness $t = 0.01$. The (unknown) exact solution is expected to be singular near the origin at the re-entering corner even though the load is uniformly distributed and the material parameters are constant (with the values from Sect. 4). We start our finite element computation with a coarse mesh shown in Fig. 2 and refine uniformly but presumably sub-optimally.

Table 2 displays the sequence of obtained and extrapolated values for the constants c_k and C_k. The energy error e_k of the finite element approximation on the mesh $\mathscr{T}_k$ were obtained with (1.3) and the extrapolated value $C_5 = 4.0609 \times 10^{-9}$.

Table 2. Numerical results in the Example of Sect. 5 for uniform mesh-refinements and $\alpha = 100$

k	N	$c_k \times 10^{-9}$	$e_k \times 10^{-5}$	$C_k \times 10^{-9}$	$\eta_k \times 10^{-5}$
1	87	1.2131	28.329		
2	339	2.8887	24.008		
3	1347	3.7112	18.240	4.5042	18.371
4	5379	4.0039	14.547	4.1657	14.595
5	21507	4.0516	9.6811	4.0609	9.6993

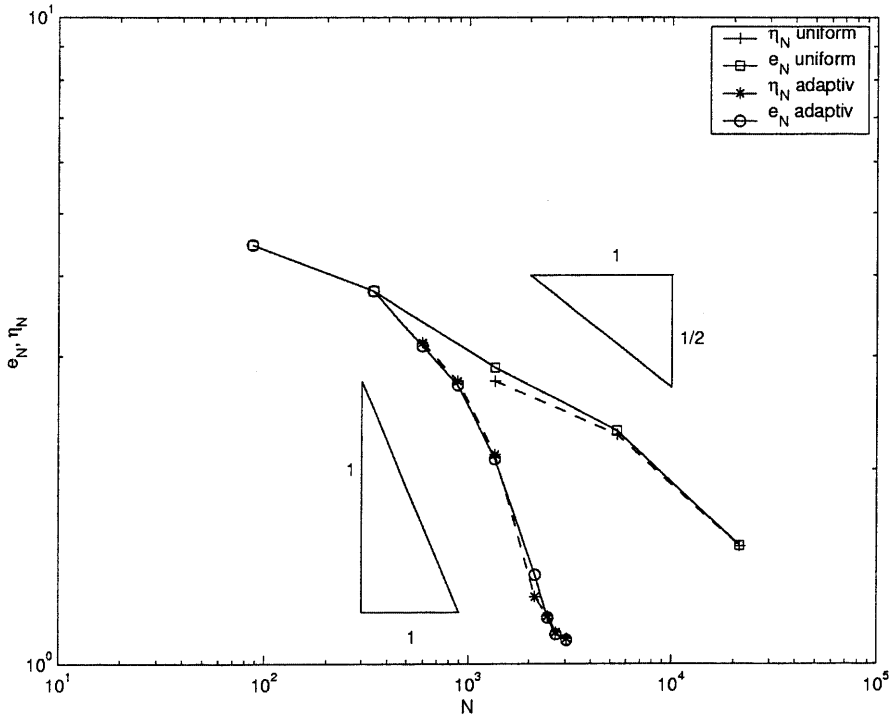

Fig. 3. Relative error versus number of degrees of freedom N for uniform and adaptive refinement in the Example of Sect. 5

Table 3. Numerical results in the Example of Sect. 5 for adapted mesh-refinements and $\alpha = 100$

k	N	$c_k \times 10^{-9}$	$e_k \times 10^{-5}$	$C_k \times 10^{-9}$	$\eta_k \times 10^{-5}$
1	87	1.2131	28.336		
2	339	2.8887	24.015		
3	591	3.5288	19.710	3.9245	19.676
4	885	3.7617	17.133	3.8949	17.084
5	1347	3.8268	13.158	3.8520	13.078
6	2131	3.8898	8.7279	5.8278	9.6874
7	2453	3.8294	7.4950	3.8590	7.3591
8	2691	3.7933	7.0633	3.7397	6.8322
9	3041	3.7755	6.9174	3.7580	6.6949

The last two columns display the error η_k calculated with c_k as explained in (iii) of Sect. 3. The convergence of the extrapolated values C_k is very fast and the resulting error estimation is very good: η_k is a very good estimate of e_k.

To assess the quality of the extrapolation for a non-uniform mesh, we employed an adaptive mesh-refining algorithm from [5]. The initial mesh $\mathcal{T}_0$ and the mesh $\mathcal{T}_9$ after 9 refinement are shown in Fig. 2. The numerical values are provided in Table 3 and obtained as corresponding values in Table 2.

A comparison of the extrapolated values C_k shows as reasonable convergence but not necessarily to the same values. As the uniform meshes may inherit asymptotic error expansions form symmetry of meshes, we regard the uniform calculation (which involves much finer meshes) as the more accurate approximation (although we have no proof for that) and computed e_k in Table 3 with the same value $C = 4.0609 \times 10^{-9}$ as in Table 2.

We observe again an accurate estimation of the energy error e_k by η_k (the values for e_k obtained with a slightly different value such as 3.7580×10^{-9} were almost the same).

To assess the improvement of adaptive mesh-refinements over a sequence of uniform meshes, Fig. 3 displays $e_N = e_k/\sqrt{C}$ and $\eta_N := \eta_k/\sqrt{C_k}$ versus the degrees of freedom N. The adaptive refining algorithms leads to a fast reduction of the error compared to the uniform refinements. This is the first numerical evidence that adaptive algorithms are superior for the Reissner–Mindlin plate and so indeed use-full tools.

References

1. **Arnold DN, Brezzi FF** (1989) Some new elements for the Reissner–Mindlin plate model. In Lions JL, Baiocchi C (eds.) Boundary Value Problems for Partial Differential Equations and Applications. Masson, pp 287–292
2. **Boffi D, Lovadina C** (1997) Analysis of new augmented Lagrangian formulations for mixed finite element schemes. Numer. Math. 75: 405–419
3. **Braess D** (1997) Finite Elemente. Springer-Verlag
4. **Brezzi F, Fortin M** (1991) Mixed and hybrid finite element methods. Springer-Verlag
5. **Carstensen C, Weinberg K** (1999) Adaptive mixed finite element method for Reissner–Mindlin plates. Mathematisches Seminar, Christian-Albrechts-Universität zu Kiel, Technical Report, 00-7
6. **Chapelle D, Stenberg R** (1998) An optimal low-order locking-free finite element method for Reissner–Mindlin plates. Math. Models and Methods in Appl. Science 8: 407–430
7. **Ciarlet PG** (1978) The finite element method for elliptic problems. North-Holland, Amsterdam
8. **Lovadina C** (1996) A new class of finite elements for Reissner– Mindlin plates. SIAM J. Numer. Anal. 33: 2457–2467
9. **Stoer J** (1989) Numerische Mathematik. Springer-Verlag
10. **Weinberg K** (1999) An adaptive finite element approach for a mixed Reissner–Mindlin plate formulation. Comput. Methods Appl. Mech. Engrg., in press